

## Refinement of the Molecular Charge Distribution in Cyanuric Acid

BY HANS DIETRICH

*Fritz-Haber-Institut der Max-Planck-Gesellschaft, 1000 Berlin 33/Dahlem, Federal Republic of Germany*

AND CHRISTIAN SCHERINGER

*Fachbereich Geowissenschaften, Universität Marburg, 3550 Marburg/Lahn, Federal Republic of Germany*

and

### Comparison of Observed and Calculated Electron Densities.

## X. Theoretical Static Difference Densities at Experimental Resolution and Theoretical Dynamic Difference Densities Perpendicular to the Molecular Plane for Cyanuric Acid

BY HERMANN MEYER, KARL-WILHELM SCHULTE AND ARMIN SCHWEIG

*Fachbereich Physikalische Chemie, Universität Marburg, 3350 Marburg/Lahn, Federal Republic of Germany*

(Received 16 December 1978; accepted 31 January 1979)

### Abstract

An empirical model of the charge-density distribution in cyanuric acid,  $C_3H_3N_3O_3$ , was refined from X-ray data. The model consists of atomic cores and charge clouds that are placed at the bonds and in the lone-pair regions. The scattering factors for the atomic cores are derived by the *L*-shell projection method. The charge clouds are approximated by Gaussian distributions and, hence, their scattering factors are also Gaussian. The density parameters are defined in bond-oriented Cartesian coordinate systems, which allows the exploitation of the chemical (and not crystallographic) symmetry of the molecule as much as possible. Thus, the number of independent density parameters in the model was reduced to 36. The results of the refinement and of quantum-chemical calculations (4-31 *G* basis) are presented as dynamic and static difference densities,  $\rho(\text{molecule}) - \rho(\text{isolated-atom model})$ . The theoretical difference densities are in good agreement with experiment except for the  $p_{\pi}^2$  region of the N atoms. The theoretical bond peaks are lower than the experimental ones.

### Introduction

Our recent refinement of the electron density distribution in decaborane (Dietrich & Scheringer, 1978) encouraged us to apply the method to cyanuric acid. We used the low-temperature X-ray data of Verschoor & Keulen (1971) [942 data except the 25 reflections

marked  $\sigma(F) = 100$ ] and based the refinement on *F*. The nuclear structure parameters, treated as constants during the refinement, were based on the neutron data of Coppens & Vos (1971). We thank Professor Coppens for his suggestion to redetermine these structure parameters from his neutron data treating the N scattering length as a variable and for sending us a listing of the neutron diffraction data containing the weights. Using the H, C, and O scattering lengths from Shull (1972) we based the refinement on  $F^2$  and corrected for isotropic extinction.

Except for the scattering length of N, the parameter changes were mostly below  $1\sigma$  and very few reached  $2\sigma$ . The N scattering length dropped by about  $4\sigma$  and its final value,  $0.929(3) \times 10^{-11}$  mm, agrees with that found by Kwick, Koetzle, Thomas & Takusagawa (1974). The resulting parameters are listed in Table 1. Coppens & Vos (1971) have shown that the temperature parameters can be adjusted to the lower temperature, at which the X-ray data had been collected, by multiplying them by a constant factor, 0.728, which corresponds to the ratio of the two temperatures. For the present work we have used a slightly smaller factor, 0.718. It was obtained according to Coppens & Vos (1971) by calculating the ratio of the sum  $\sum U_{ii}$  (high-order X-ray; from Table 5 of Coppens & Vos, 1971) divided by the sum  $\sum U_{ii}$  (neutron; from our Table 1).

With the new nuclear parameters and the 942 X-ray data we calculated several *X-N* sections for comparison with our molecular model. They are shown in Figs. 1 and 2. The scattering factors used for the

Table 1. *Refinement of the parameters of cyanuric acid with the neutron data of Coppens & Vos (1971)*

The H, C, and O scattering lengths used were those of Shull (1972) and the N scattering length was included as a variable. Refinement was based on  $F^2$  with an isotropic-extinction correlation. Final  $R(F) = 0.0314$ ,  $R(F^2) = 0.0325$ ,  $R_w(F^2) = 0.0478$ . E.s.d.'s in parentheses are in terms of the last decimal place. The e.s.d.'s of the scattering lengths of H, C, O are taken from Shull (1972). Anisotropic thermal parameters are  $\times 10^4 \text{ \AA}^2$ .

	$b \times 10^{11} \text{ mm}$	$x$	$y$	$z$	$U_{11}$	$U_{22}$	$U_{33}$	$U_{12}$	$U_{13}$	$U_{23}$
H(1)	-0.3740 (3)	0.25	-0.14083 (19)	0.25	378 (7)	132 (5)	270 (6)	-	242 (5)	-
C(1)	0.6648 (3)	0.25	0.41794 (8)	0.25	163 (2)	72 (2)	136 (2)	-	113 (2)	-
N(1)	0.9287 (27)	0.25	0.01139 (6)	0.25	179 (2)	77 (2)	111 (2)	-	111 (1)	-
O(1)	0.5803 (6)	0.25	0.59830 (10)	0.25	291 (4)	77 (3)	235 (3)	-	201 (3)	-
H(2)	-0.3740 (3)	0.24220 (17)	0.38422 (15)	0.07361 (11)	364 (5)	194 (4)	248 (4)	-2 (3)	234 (4)	33 (3)
C(2)	0.6648 (3)	0.24525 (6)	0.10590 (6)	0.14622 (4)	140 (2)	87 (2)	103 (2)	-3 (1)	91 (1)	-2 (1)
N(2)	0.9287 (27)	0.24454 (5)	0.30901 (5)	0.15043 (3)	185 (1)	84 (1)	133 (1)	-2 (1)	123 (1)	6 (1)
O(2)	0.5803 (6)	0.24268 (9)	0.01371 (7)	0.05714 (5)	216 (2)	102 (2)	139 (2)	-9 (2)	143 (2)	-11 (1)

(neutral) C, N, O atoms were those derived by Stewart (1970) with the  $L$ -shell projection method (SCF AO's).

The section along the molecular plane (Fig. 1) shows slightly better resolution in the lone-pair region than that of Coppens & Vos (1971). A more pronounced deviation is the minimum close to N(1) inside the ring. In order to clarify the discrepancy we recalculated the  $X$ - $N$  section with Coppens & Vos's (1971) original nuclear parameters, but it also showed the minimum at N(1). The minimum also appeared in an  $X$ - $N$  map calculated with the total set of Verschoor & Keulen's (1971) data [including the 25 reflections marked  $\sigma(F) = 100$ ].

To make possible a comparison between experimental and theoretical difference densities, the results of a 4-31  $G$  calculation for an isolated cyanuric acid molecule are included in this paper.

### The model of the molecular charge distribution

The type of model which we use was described by Dietrich & Scheringer (1978). Here we sum up its main features. The model consists of atomic cores and separate charge clouds which are placed into the bonds and at the positions of the lone-pair electrons. The scattering factors for the atomic cores are derived from Stewart's (1970)  $L$ -shell-projection-method scattering factors based on SCF AO's (the scattering factors based on STO AO's gave less satisfactory results). For the cores of the H atoms Dietrich's (1976) scattering factors are used. Thus, for an atomic core only one (charge) parameter arises in the refinement. The excess charge clouds between the nuclei are approximated by three-dimensional Gaussian distributions. Hence, their scattering factors are also Gaussian. For each charge cloud a Cartesian coordinate system is set up with respect to which the density parameters are defined. These are: one charge ( $q$ ), three positional coordinates ( $X, Y, Z$ ) and three principal components ( $V_{11}, V_{22}, V_{33}$ )

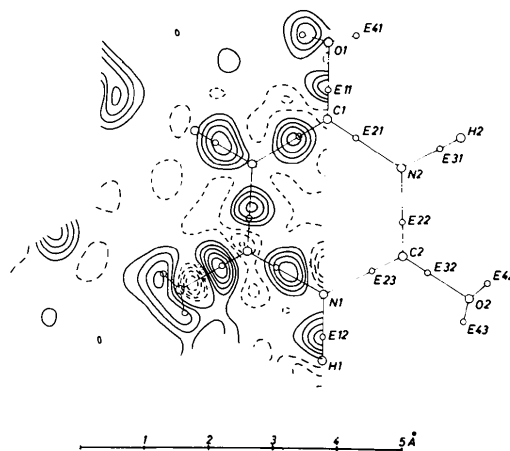


Fig. 1.  $X$ - $N$  section in the plane of the ring. On the right-hand side numbering of atoms and charge clouds of our empirical charge-density model are shown. Contour interval  $0.1 \text{ e \AA}^{-3}$ , positive contours are full lines, the zero contour is dotted, negative contours are dashed.

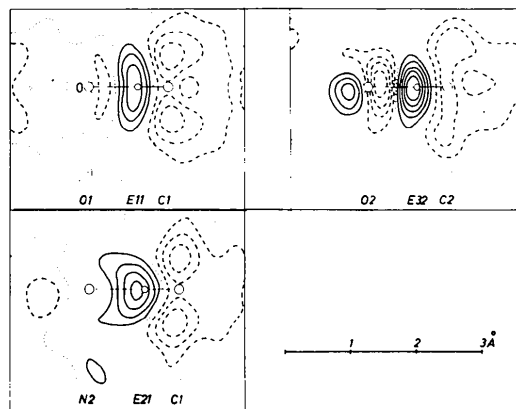


Fig. 2.  $X$ - $N$  sections perpendicular to the ring plane along three bonds having  $\pi$  character. Contours are as in Fig. 1.

of the smearing tensor. Since the axes of the coordinate system are directed towards the principal directions of the bond, it appears to be justified to use zero values for the off-diagonal components of the smearing tensor. Thus, for each charge cloud there are seven parameters at the most. Our model of the charge distribution in cyanuric acid is illustrated in Figs. 1, 3, 4 and 5.

The description of the charge distribution by means of bond-oriented coordinate systems allows us to exploit the chemical symmetry of the molecule as much as possible. This is done by application of constraints (which can now be easily formulated) and thus the number of independent parameters is reduced. Since in the crystal the hydrogen bridges between the molecules

are all of about equal strength and differ mainly with respect to their geometry (Coppens & Vos, 1971), we set the C–N groups equivalent and similarly the N–H bonds for which, in addition, rotational symmetry was assumed. From the  $X$ -N synthesis it was clear that the O atoms could not be set equivalent. But we assumed the symmetry  $m$  with respect to the molecular plane, and with respect to the planes along the C–O bonds, perpendicular to the molecular plane. The constraints imposed on the parameters can be seen from Table 2. The number of independent density parameters in our model is 36, whereas the maximum possible number is 78 (for eight atomic cores and ten charge clouds). We consider the reduction of the number of parameters as an important advantage for the refinement of the model.

The vibration tensors for the bond charges were taken to be the weighted average of the vibration tensors of the nuclei [eq. (3) of Dietrich & Scheringer (1978)]. Hence, they are somewhat too large, but the error introduced in the difference density is not likely to exceed  $0.1 \text{ e } \text{Å}^{-3}$  (Scheringer, 1977). The vibration tensors for the lone-pair charge clouds  $E(41)$ ,  $E(42)$ , and  $E(43)$  are set equal to those of the respective O nuclei. The positional parameters of the nuclei and all thermal parameters are fixed quantities in the refinement; the scale factor is the only non-density parameter that is refined. In order to constrain the total charge of the unit cell to zero we introduced  $F(000)$  as an observed quantity with high statistical weight (Harel & Hirshfeld, 1975).

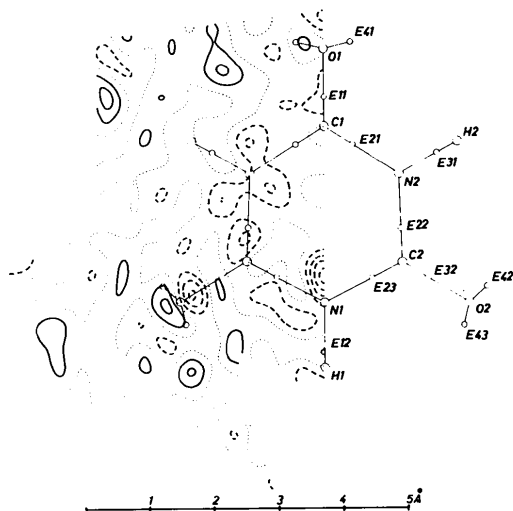


Fig. 3.  $F_o - F_c$  section in the plane of the ring. Contours are as in Fig. 1.

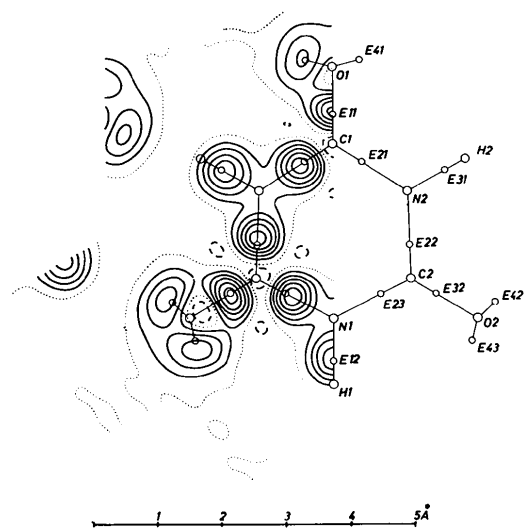


Fig. 4.  $(M - A)_{\text{dyn}}$  section in the plane of the ring. Contours are as in Fig. 1.

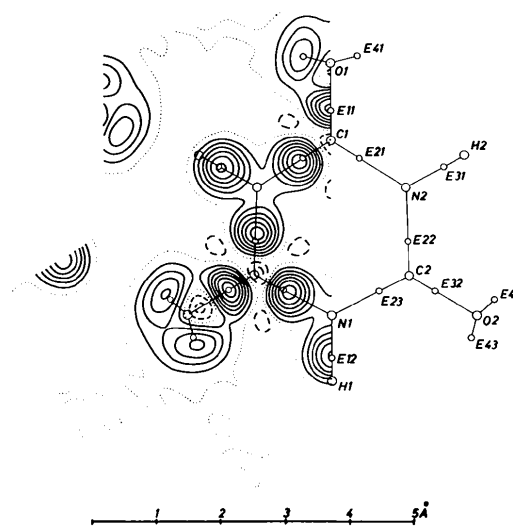


Fig. 5.  $(M - A)_{\text{stat}}$  section in the plane of the ring. Contours are as in Fig. 1.

## Results of the refinement

The values obtained in the refinement are listed in Table 2. The thermal parameters of the charge clouds are not

Table 2. *Charge-density parameters for cyanuric acid*

Nuclear positions and vibration tensors are based on the neutron data of Coppens & Vos (1971). The refinement with 90 K X-ray data of Verschoor & Keulen (1971) is based on  $F$ . Final  $R(F) = 0.0277$ . E.s.d.'s in parentheses are in terms of the last decimal place.

Centre	Charge $q$ (e)	Reference atoms		Positional parameters		Smearing parameters $\times 2\pi^2$ ( $\text{\AA}^2$ )		
		$A_1$	$A_2$	Distance ( $\text{\AA}$ ) $r(E_i - A_1)$	Angle ( $^\circ$ ) $E_i - A_1 - A_2$	$V_{11}$	$V_{22}$	$V_{33}$
H(1)	as H(2)							
C(1)	as C(2)							
N(1)	as N(2)							
O(1)	0.21 (22)							
H(2)	0.35 (4)							
C(2)	1.81 (14)							
N(2)	-0.24 (4)							
O(2)	0.56 (27)							
$E(21)$	-0.46 (4)	N(2)	C(1)	0.847 (9)		2.39 (14)	1.57 (8)	1.32 (9)
$E(22)$	as $E(21)$	N(2)	C(2)					
$E(23)$	as $E(21)$	N(1)	C(2)					
$E(11)$	-0.53 (5)	O(1)	C(1)	0.752 (13)		2.95 (26)	1.78 (19)	1.05 (14)
$E(32)$	-0.52 (5)	O(2)	C(2)	0.756 (11)		2.59 (18)	1.75 (13)	0.96 (11)
$E(12)$	as $E(31)$	H(1)	N(1)					
$E(31)$	-0.15 (2)	H(2)	N(2)	0.365 (17)		1.17 (17)	as $V_{11}$	0.81 (20)
$E(41)$	-0.29 (10)	O(1)	C(1)	0.430 (65)	104 (4)	2.26 (29)	2.93 (47)	1.42 (41)
$E(42)$	-0.42 (11)	O(2)	C(2)	0.368 (47)	107 (3)	2.17 (15)	2.59 (21)	1.65 (28)
$E(43)$	as $E(42)$	O(2)	C(2)					

given; they can easily be calculated from the thermal parameters of the nuclei [eq. (3) of Dietrich & Scheringer (1978)].

$R(F)$  for 942 data and 37 parameters is 0.0277. [ $R(F)$  for the isolated-atom model with the same positional and thermal parameters, and a refined scale factor, is 0.0438.]  $R(F) = 0.0277$  for 37 parameters compares well with the results of Jones, Pautler & Coppens (1972): they obtained  $R = 0.030$  for 49,  $R = 0.031$  for 44, and  $R = 0.026$  for 62 parameters in various models. Kutoglu & Hellner (1978) obtained  $R = 0.0252$  for a model with 140 parameters.

The e.s.d.'s for the parameters (Table 2) are calculated from the full inverse matrix, and some are large. This is a consequence of the resolution limit of the X-ray data, 0.62  $\text{\AA}$ , which leads to correlations between parameters of charge units which are closer together. Column 5 of Table 2 shows distances down to about 0.4  $\text{\AA}$  which should be the resolution limit one would actually need. With the use of constraints we have overcome much of the correlation problem but could not solve it totally. The e.s.d. of the difference density,  $\rho_o - \rho_c$ , was calculated as  $\sigma(\Delta\rho) = 0.056 \text{ e } \text{\AA}^{-3}$  [cf. Rees (1976) eqs. 1 and 10], where  $\sigma(\rho_c)$  and the scale-factor term  $\sigma(k)/k$  were neglected.

The results of the refinement are presented in two different ways. (1) We have calculated the  $F_o - F_c$  synthesis in the plane of the molecule (Fig. 3) and some sections perpendicular to it (Fig. 6) in order to obtain a criterion for the fit of our model to the experimental data. (2) For a direct display of our model and for

comparison with other work and theoretical calculations we have computed corresponding sections of the dynamic difference density

$$\rho[\mathbf{x}(M - A)_{\text{dyn}}] = \frac{1}{V} \sum_{\mathbf{h}} [F_c(M, \mathbf{U}) - F_c(A, \mathbf{U})] \times \exp(-2\pi i \mathbf{h} \mathbf{x}),$$

(Figs. 4 and 7), and the static difference density

$$\rho[\mathbf{x}(M - A)_{\text{stat}}] = \frac{1}{V} \sum_{\mathbf{h}} [F_c(M, \mathbf{U} = \mathbf{O}) - F_c(A, \mathbf{U} = \mathbf{O})] \exp(-2\pi i \mathbf{h} \mathbf{x})$$

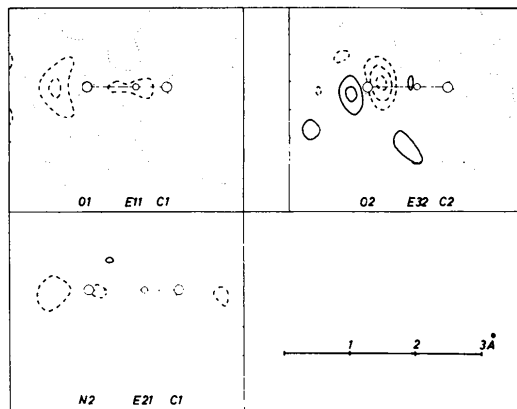


Fig. 6.  $F_o - F_c$  sections perpendicular to the ring plane, corresponding to Fig. 2. Contours are as in Fig. 1.

(Figs. 5 and 8), with structure factors included up to the limit of the experimental resolution.

The good fit of our model to the data becomes especially obvious if one compares the dynamic difference density (Figs. 4 and 7) with the corresponding  $X-N$  sections (Figs. 1 and 2).

The  $F_o - F_c$  synthesis (Figs. 3 and 6) provides a more critical test. It shows that there are a few systematic deviations:

- (1) The minimum and the maximum at O(2).
- (2) A systematic pattern of small minima ( $-0.2 \text{ e } \text{\AA}^{-3}$ ) around the N atoms in the prolongation of all C-N and H-N bonds.
- (3) The deeper minimum in the prolongation of H(1)-N(1) ( $-0.4 \text{ e } \text{\AA}^{-3}$ ).

(1) is mostly a consequence of the fact that, in our empirical model, the polarization of the O atoms in the C=O bond direction has not explicitly been accounted for. In the concept of our model a polarization term would be composed of a positive charge cloud close to the O atom on the O=C bond axis and its negative equivalent at the same distance on the other side of the

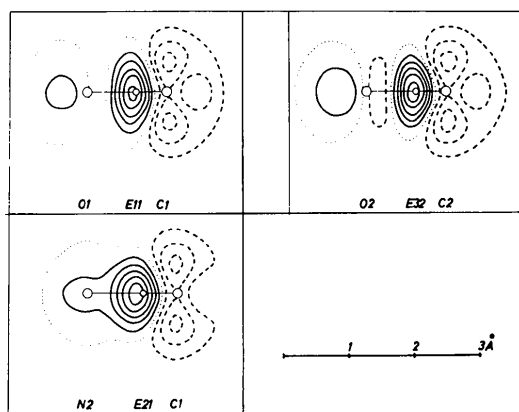


Fig. 7.  $(M - A)_{\text{dyn}}$  sections perpendicular to the ring plane, corresponding to Fig. 6. Contours are as in Fig. 1.

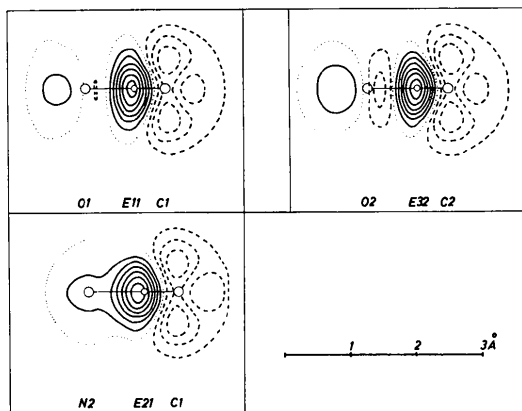


Fig. 8.  $(M - A)_{\text{stat}}$  sections perpendicular to the ring plane, corresponding to Fig. 7. Contours are as in Fig. 1.

O atom. If isotropic smearing is assumed only three additional parameters would be needed, *i.e.* the distance from the O atom, one charge and one smearing parameter. But the substantial overlap of the two polarizing charge clouds with the O core and the lone-pair ellipsoids causes severe correlation between the parameters of these five closely packed charge units because of the resolution limit of the X-ray data. For this reason we did not refine a model containing polarization terms for the O atoms. As a consequence, the polarization is at least partially compensated for by an increase of the positive charge of the O cores, an increase of the negative charge clouds representing the lone-pair electrons, and a decrease of the distance between O and its lone-pair clouds. Since the polarization of O(1) is much smaller than that of O(2) the tendency for these compensation effects can be recognized by comparison of the relevant parameters in Table 2 although these parameters have particularly high e.s.d.'s due to correlation. The  $F_o - F_c$  section in Fig. 3 shows that the compensation is complete for O(1) but not for O(2).

The asymmetry of the maximum at O(2) in the  $F_o - F_c$  map (Fig. 3) and the corresponding asymmetry of the lone-pair charge distribution in the  $X-N$  section in Fig. 1 suggest that the lone-pair clouds  $E(42)$  and  $E(43)$  should not be equivalent as assumed in our model.  $E(42)$  should contain more charge than  $E(43)$  which is plausible also from the chemical point of view since  $E(42)$  lies approximately on the hydrogen bridge  $O(2) \cdots H'(2)$ .

The  $F_o - F_c$  sections show that all the other constraints in our model proved to be valid within the limits of error.

(2) The pattern of small minima around the N atoms (and another feature in the C-N bonds which will be discussed below) seems to indicate that the optimal representation of the N cores in our model has not yet been found. The model could be altered by introducing small positive charge clouds in the indicated positions. But even if the additional charge clouds were constrained to have all the same charge, the same distance from N, and isotropic smearing (which would lead to a total of three additional parameters), considerable interaction with the N charge parameter is to be expected. An alternative possibility to reduce the density of our model in the region where the minima appear seemed to be the use of less-diffuse N cores. This should at the same time reduce the asymmetry of the C-N bond peaks which are shifted towards the C atoms, as can be seen best from the static difference sections in Figs. 5 and 8. The  $X-N$  sections do not indicate such an asymmetry. Several refinements with N cores whose peripheral density was contracted to various degrees failed. The failure is, however, plausible from the physical point of view. Since the N cores have a negative charge (Table 2) they should be more diffuse rather than more compact compared to the neutral

atom. Coppens (1977) suggested an expansion/contraction parameter  $\kappa$  for the  $L$ -shell projection method. In an application to cyanuric acid he found net charges of 0.4 e and  $\kappa = 0.961$  (5) for the N atoms. The  $\kappa$  value corresponds to a considerable expansion of the N  $L$ -shell. To estimate the net charges for the N atoms in our model one may add half the N–C and the N–H bond clouds to the N core charge of  $-0.24$  e (Table 2). The resulting value,  $-0.78$  e, is twice as high as that from Coppens's (1977) one-centre refinement. Similarly one obtains from Table 2 net charges for C, O(1), and O(2) which are too high, namely  $+1.09$ ,  $-0.64$ , and  $-0.54$  e respectively. These high net charges of all atoms (except H) are probably the reason for the minima around the N atoms and the asymmetry of the C–N bond clouds. We suppose that there would be a good chance to lower the net atomic charges by introducing  $\kappa$  parameters for the valence shells of all atomic cores in our model.

(3) The minimum close to N(1) seems to be caused by the unusual type of linear hydrogen bridge N(1)–H(1)···O'(1)=C'(1).

The  $\pi$  character of the C–N and C=O bonds is well represented by our model as can be seen from Figs. 2, 6, 7, and 8. A rather surprising feature in Figs. 2, 7, and 8 is that they show minima above and below the C atoms, *i.e.* in the C  $p_\pi^2$  region. This result is in agreement with an orbital product population analysis of Coppens, Csonka & Willoughby (1970) in which very low population parameters for the  $p_\pi^2$  products were obtained. Similar minima were found in difference syntheses by Verschoor & Keulen (1971), though flatter and shifted away from the atoms.

#### Comparison with experimental difference densities obtained by other authors

Our  $(M-A)_{\text{dyn}}$  section in Fig. 4 may be compared with the corresponding population asphericity maps of Jones, Pautler & Coppens (1972). The maps computed from their models I-H (62 parameters) and II-H (49 parameters) which are based on Hartree-Fock functions show the best agreement. A general difference seems to be that in our sections the nuclear positions of N and C appear on a somewhat higher density level, as in the  $X-N$  map.

Finally our model may be compared with that refined by Kutoglu & Hellner (1978). A presentation of this model in the form of dynamic and static difference densities, corresponding to our Figs. 4 and 5, was given by Scheringer, Kutoglu, Hellner, Hase, Schulte & Schweig (1978) and by Scheringer, Kutoglu & Hellner (1978). The C–N and C–O bond peaks obtained by these authors are lower by about two lines ( $0.2 \text{ e } \text{Å}^{-3}$ ), the lone-pair peaks are lower by about one line and the minima at the O atoms are deeper by about three lines.

The differences appear to be due to an inadequacy of the Kutoglu & Hellner (1978) model and the fact that the positional and thermal parameters of the atoms were also determined from the X-ray data. A more detailed discussion of this subject will be published (Kutoglu & Scheringer, 1979).

#### Comparison with theoretical difference densities

Scheringer, Kutoglu, Hellner, Hase, Schulte & Schweig (1978) presented the theoretical static difference density at infinite resolution [obtained with the 4-31  $G$  basis set of Ditchfield, Hehre & Pople (1971)] in the plane of the molecule as well as the corresponding dynamic density [determined with the smearing procedure of Hase, Reitz & Schweig (1976)]. In Fig. 9 we supplement these densities by the static difference density at experimental resolution [0.62 Å; for the method of calculation see Hase, Reitz & Schweig (1976)]. To enable comparison between theoretical and

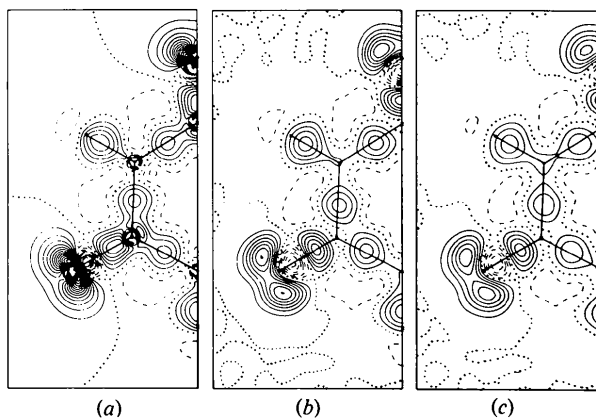


Fig. 9. Theoretical  $M-A$  sections in the molecular plane. Contours are as in Fig. 1. (a) Static with infinite resolution. (b) Static with the resolution of the X-ray data, 0.62 Å. (c) Dynamic.

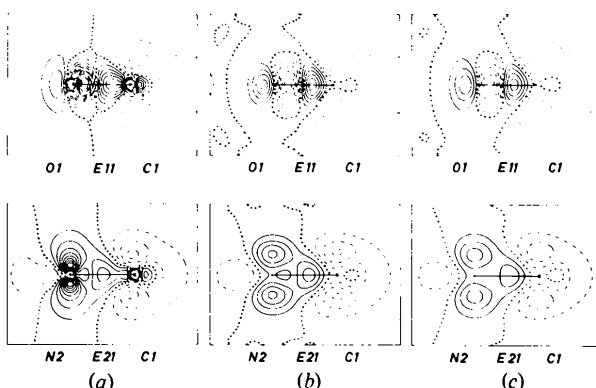


Fig. 10. Theoretical  $M-A$  sections perpendicular to the molecular plane. Contours are as in Fig. 1. (a) Static with infinite resolution. (b) Static with the resolution of the X-ray data, 0.62 Å. (c) Dynamic.

experimental densities in sections perpendicular to the plane of the molecule we calculated all three types of densities in the planes specified in Fig. 10.

Comparison between the various types of theoretical and experimental densities reveals: firstly, the overall picture of difference densities is markedly influenced by series termination. A false account of this effect led Scheringer, Kutoglu & Hellner (1978) to underestimate in their experimental static difference density at infinite resolution the peak heights for the lone-pair peaks of the O atoms (estimated to be  $0.4 \text{ e } \text{Å}^{-3}$ ) and thus to underrate the agreement with the corresponding theoretical value ( $1.4 \text{ e } \text{Å}^{-3}$ ). Secondly, there is good overall agreement of the theoretical (Figs. 9 and 10) and experimental (Figs. 1, 2, 4, 5, 7 and 8) shapes of the densities, with one notable exception. Theory predicts appreciable density with peak heights of  $0.3$  to  $0.4 \text{ e } \text{Å}^{-3}$  in the  $\pi$  regions of the N atoms which is completely missing in the experimental densities. Finally, the calculated peak heights are  $0.1 \text{ e } \text{Å}^{-3}$  lower in the C=O and N-H bonds,  $0.2$  to  $0.3 \text{ e } \text{Å}^{-3}$  lower in the C-N bond, and  $0.1$  to  $0.2 \text{ e } \text{Å}^{-3}$  higher in the lone-pair region than the observed peak heights. These shortcomings of the  $4\text{-}31 \text{ G}$  basis set could be remedied by including bond-polarization functions (Hase & Schweig, 1977; Meyer & Schweig, 1979) in the basis set.

### Conclusion

With our empirical model a good fit to the X-ray data was obtained. Also noticeable is the good agreement of the empirical  $(M - A)_{\text{dyn}}$  density with the  $X$ - $N$  map. The agreement of the empirical densities with the theoretical densities is good, except for the C-N bond peaks, the region around the O atoms and the  $p_{\pi}$  regions of the N atoms. That the theoretical C-N bond peaks are lower by  $0.2$ – $0.3 \text{ e } \text{Å}^{-3}$  is considered to be due to a deficiency of the theoretical model. On the other hand, the stronger polarization of the O atoms shown in the theoretical density is more likely to be correct since the polarization was not successfully treated with the empirical model (due to limited resolution). The zero density in the  $p_{\pi}$  region of the experimental maps (as opposed to pronounced peaks in the theoretical maps) may, perhaps, be ascribed to the strong hydrogen bonds present in the crystal which are neglected in the theoretical calculation. Similarly, the non-equivalence of the lone pairs at O(2) (which has been neglected in the empirical model and, of course,

also in the theoretical model) may be a consequence of the geometry of the hydrogen bond  $\text{O}(2) \cdots \text{H}(2)'$ , with the lone pair  $E(42)$  approximately on the line  $\text{O}(2) \cdots \text{H}(2)'$ .

We consider the fact that an empirical model, which only requires 36 density parameters, could be fitted so well to the X-ray data and yielded results in good agreement with other work indicates that its concept is adequate. The representation of the atomic cores in our model could probably be improved by introducing  $\kappa$  parameters (Coppens, 1977) for the valence shells of all atoms.

We thank the Deutsche Forschungsgemeinschaft for support of this work.

### References

- COPPENS, P. (1977). *Isr. J. Chem.* **16**, 159–162.  
 COPPENS, P., CSONKA, L. & WILLOUGHBY, T. V. (1970). *Science*, **167**, 1126–1128.  
 COPPENS, P. & VOS, A. (1971). *Acta Cryst.* **B27**, 146–158.  
 DIETRICH, H. (1976). *Acta Cryst.* **A32**, 347–348.  
 DIETRICH, H. & SCHERINGER, C. (1978). *Acta Cryst.* **B34**, 54–63.  
 DITCHFIELD, R., HEHRE, W. J. & POPLE, J. A. (1971). *J. Chem. Phys.* **54**, 724–728.  
 HAREL, M. & HIRSHFELD, F. L. (1975). *Acta Cryst.* **B34**, 162–172.  
 HASE, H. L., REITZ, H. & SCHWEIG, A. (1976). *Chem. Phys. Lett.* **39**, 157–159.  
 HASE, H. L. & SCHWEIG, A. (1977). *Angew. Chem.* **89**, 264–265; *Angew. Chem. Int. Ed. Engl.* **16**, 258–259.  
 JONES, D. S., PAUTLER, D. & COPPENS, P. (1972). *Acta Cryst.* **A28**, 635–645.  
 KUTOGLU, A. & HELLNER, E. (1978). *Acta Cryst.* **B34**, 1617–1623.  
 KUTOGLU, A. & SCHERINGER, C. (1979). *Acta Cryst.* **A35**, 458–462.  
 KVICK, A., KOETZLE, T. F., THOMAS, R. & TAKUSAGAWA, F. (1974). *J. Chem. Phys.* **60**, 3866–3874.  
 MEYER, H. & SCHWEIG, A. (1979). To be published.  
 REES, B. (1976). *Acta Cryst.* **A32**, 483–488.  
 SCHERINGER, C. (1977). *Acta Cryst.* **A33**, 426–429, 430–433.  
 SCHERINGER, C., KUTOGLU, A. & HELLNER, E. (1978). *Acta Cryst.* **B34**, 2670–2671.  
 SCHERINGER, C., KUTOGLU, A., HELLNER, E., HASE, H. L., SCHULTE, K. W. & SCHWEIG, A. (1978). *Acta Cryst.* **B34**, 2162–2165.  
 SHULL, C. (1972). *Mass. Inst. Technol. Neutron Diffr. News Lett.* p. 20.  
 STEWART, R. F. (1970). *J. Chem. Phys.* **53**, 205–213.  
 VERSCHOOR, G. C. & KEULEN, E. (1971). *Acta Cryst.* **B27**, 134–145.